Photocaged FLP Recombinase for Precise Spatio-temporal Control of Gene Expression

Jose Javier Vazquez Rodriguez, Kieran Baxter, and Sebastian Greiss*

Institute for Neuroscience and Cardiovascular Research, University of Edinburgh, United Kingdom
*Correspondence: S.Greiss@ed.ac.uk

ABSTRACT

The ability to precisely control gene expression is fundamental to studying biological processes. Using site-specific recombinases such as Cre or FLP, gene expression can be controlled, albeit with limited spatiotemporal precision, dictated by the expression profile of the promoters used to drive them. Here we develop a photocaged FLP recombinase which can be efficiently and precisely controlled using light. To achieve this, we replace critical amino acid residues in the FLP active site with their photocaged counterparts using genetic code expansion technology. We find that photocaged FLP displays no detectable background activity and can be activated by brief illumination in the range of milliseconds to seconds. We further demonstrate that photocaged FLP can be activated using a standard 405 nm microscope-mounted laser, allowing for control of gene expression with single-cell precision.

INTRODUCTION

Methods to control gene expression are fundamental to studying biological processes in living systems. Such methods include the use of tissue-specific promoters or of extraneous transcription factors such as Gal4 to drive the expression of target genes[1]. Another widely used approach involves site specific DNA recombinases (SSR) such as Cre or FLP, which can remodel DNA to switch the expression of target genes on or off[2]. However, spatial and temporal targeting of SSR systems depends on the availability of promoters to drive SSR expression. This is limiting as often promoters with desirable spatial and temporal expression profiles for an experiment do not exist. Several strategies have been employed to overcome this limitation. Temporal control can be achieved through chemically inducible systems, for example using tamoxifen[3], or by employing heat-shock inducible promoters[4]. Spatial control can be improved through the use of overlapping promoter pairs to express individual components of the system[5].

More recently, approaches to optically control the activity of SSRs have been developed. Optical activation is non-invasive and has the potential to offer unmatched spatial and temporal control. Most approaches for imparting optical responsiveness to SSRs involve split proteins that are reassembled using photodimerizers such as LOV domains[6]. While this approach has been applied for Cre[7] and FLP[6] recombinases, it is often accompanied by background activity in the 'off' state, and low efficiency in the 'on' state. Additionally, its practical utility is hindered by the requirement for prolonged light exposure to induce recombinase reconstitution, and the use of wavelengths in the visible spectrum which overlap with wavelengths often used for imaging and optogenetic applications.

An alternative approach for optically controlling SSR activity involves the incorporation of photocaged amino acids into the enzyme's active site in place of essential catalytic residues using genetic code expansion (GCE) technology[8]. Here, a photolabile caging group attached to the ncAA side-chain blocks activity of the enzyme, until brief illumination removes the caging group and restores protein activity. This approach has been successful for Cre, which has been photocaged using photocaged variants of tyrosine to replace the active site Tyr324[9,10], and photocaged variants of lysine to replace the active site Lys201[10–12]. The use of photocaged amino acids has several advantages: the photocaging groups are stable at wavelengths commonly used for imaging and other optogenetic applications; photocaged Cre (PC-Cre) shows no background activity prior to illumination; activation can be achieved with sub-second illumination time; and the light can be precisely targeted to individual cells, thereby allowing the control of gene expression with single-cell precision[12]. PC-Cre has been successfully applied in single-celled systems[9,10] as well as in animals such as zebrafish[11] and *C. elegans*[12].

Several SSRs besides Cre exist and have been employed to control gene expression in cells and multicellular organisms[2]. The most widely used among these is flippase (FLP), originally derived from the 2 μ plasmid of *S. cerevisiae*[13]. Compared to Cre, FLP is more active at the lower body temperatures of fish, worms, and flies[14]. At the same time, versions of FLP with improved activity and stability at 37 °C for use in mammalian systems have been developed[15]. Furthermore, while Cre can be toxic to cells[16], no such deleterious effects have been reported for FLP[17].

Here, we develop photocaged FLP (PC-FLP) by replacing specific tyrosine, lysine, and cysteine residues in its active site with photocaged variants. We find that FLP can be photocaged with no background activity and that it can be activated with up to 100% efficiency upon illumination. We also find that in *C. elegans,* PC-FLP is more efficient than PC-Cre. Furthermore, we have identified PC-FLP variants with improved activation efficiency at longer wavelengths and demonstrated efficient activation using a standard 405 nm microscope-mounted laser, enabling the control of gene expression with single cell precision in *C. elegans*.

RESULTS

Strategy for photocaging FLP recombinase

To photocage FLP, we used genetic code expansion, which enables the cellular translational machinery to utilise, and incorporate into proteins, non-canonical amino acids (ncAAs) with properties not found in nature. This is achieved by expressing an orthogonal aminoacyl-tRNA-synthetase (aaRS)/tRNA pair in the cell. The aaRS specifically recognises the ncAA and attaches it to its cognate tRNA, which in turn delivers it to the ribosome where it is incorporated into the nascent polypeptide chain in response to a designated "unassigned" codon, most commonly a UAG (amber) stop codon (**Fig. 1a**). Here we utilise the pyrrolysyl-tRNA-synthetase (PylRS)/tRNA(Pyl) pair from the archaeon *Methanosarcina mazei*, which is highly efficient in eukaryotic cells and the most commonly used pair in in multicellular organisms[18].

To qualify as a target for photocaging, a residue in an enzyme needs to fulfil two criteria: installing the photocaged ncAA must abolish enzymatic activity, and removal of the caging group must restore activity. To select residues for photocaging FLP that fulfil these criteria, we first compared its structure to that of Cre, which has previously been successfully photocaged.

Although Cre and FLP share only 13% sequence identity and assemble their active sites differently, both belong to the tyrosine recombinase family and therefore contain the conserved catalytic pentad[2], which includes the residues K201 and Y324 at which Cre has previously been photocaged. These residues are conserved in FLP as K223 and Y343[2,19]. Therefore, we investigated K223 and Y343 as targets for installing optical control in FLP by replacing them with their photocaged counterparts.

In addition to the conserved catalytic tyrosine and lysine residues that are shared between FLP and Cre, we also identified C189 that is present in FLP, but not in Cre, as a photocaging target. FLP belongs to the family of yeast-derived tyrosine recombinases, which share between them greater sequence conservation than FLP does with Cre and contain several invariant residues. C189 is one of these invariant residues, located within the active site of FLP, and which if mutated to arginine or tryptophan results in a complete loss of function[20]. We have previously shown that the photocaged cysteine PCC2 can be efficiently incorporated in *C. elegans* using the evolved PylRS variant PCC2RS[21,22]. Thus, we chose C189 as another promising candidate residue for photocaging the activity of FLP.

To express and assay each of the photocaged FLP (PC-FLP) variants, we generated transgenic *C. elegans* strains each expressing a different FLP construct, containing an amber stop codon at the position that corresponds to the ncAA incorporation site (**Fig. 1b**, **Supplementary Table 1**). Along with the FLP construct, we co-transformed the genetic code expansion machinery components, namely a PylRS variants evolved to recognise the respective photocaged ncAA and optimised for use in eukaryotic cells by the addition of a N-terminal nuclear export signal[12,23], and tRNA(M15)$_{CUA}$, a previously optimised pyrrolysyl tRNA[12,24] to decode the amber stop codon present in FLP (**Fig. 1b**). Expression of the PylRS and FLP variants was driven by the promoter for the glutamate receptor *glr-1* that is active in a subset of *C. elegans* head neurons[12]. To visualise presence of the expression construct in our transgenic lines, we co-expressed red fluorescent mKate2 in an artificial operon with FLP. The FLP gene was modified along the lines of our previously published optimised PC-Cre by adding a C-terminal nuclear localisation signal (NLS) derived from *C. elegans egl-13*[12]. The C-terminal NLS ensures that only full length FLP is actively transported to the nucleus. As a reporter to visualise FLP activity we co-transformed a construct consisting of a Citrine2 gene separated from its promoter by a transcriptional terminator flanked by two FRT sites. FLP activity would thus result in excision of the transcriptional terminator and expression of the fluorescent Citrine2 (**Fig. 1c**). To drive expression of the Citrine2 reporter we used the promoter of *C. elegans maco-1*, which is active pan-neuronally[12].

Using this strategy, namely transgenic animals that co-express FLP constructs containing an amber stop codon in the selected position, the genetic code expansion machinery components, and the reporter system for visualising recombinase activity, we assessed the photocaging efficiency in the three selected FLP residues.

Photocaging FLP at Tyrosine 343

To photocage FLP at the catalytic Y343, we tested three different photocaged tyrosine variants. The photocaged tyrosine ortho-nitro-benzyl tyrosine (ONBY), which was previously used to photocage Cre[10], and the photocaged tyrosine variants nitropiperonyl-tyrosine (NPY) and methyl-nitropiperonyl-tyrosine (MNPY). NPY and MNPY show improved uncaging characteristics compared to ONBY[25], but have thus far not been used for photocaging either Cre or FLP. We have previously shown that these photocaged tyrosine variants

can be efficiently incorporated in *C. elegans* using the evolved PylRS variant NPYRS[25,26]. We therefore evaluated their suitability for photocaging the activity of FLP recombinase.

We generated transgenic *C. elegans* strains by co-expressing NPYRS, tRNA(M15)$_{CUA}$, the FLP construct containing an amber stop codon at position Y343, and the Citrine2 reporter to visualise activity of the recombinase.

To assay activation of PC-FLP using the photocaged tyrosine variants, transgenic animals were grown from the L1 larval stage for 24 hours on Nematode Growth Medium (NGM) agar plates supplemented with 1 mM of either NPY, ONBY, or MNPY, followed by illumination with 365 nm light. 24 hours after illumination we observed strong Citrine2 fluorescence in animals grown in the presence of any of the three photocaged tyrosine variants (**Fig. 2c**), indicating that the function of FLP was restored after illumination. We observed activation efficiencies following illumination of 99.1% 99.5% and 98.5% for PC-FLP photocaged with NPY, ONBY, or MNPY respectively (**Fig. 3a**). In contrast, we saw no Citrine2 expression in animals grown on any of the photocaged tyrosine variants but not illuminated, indicating that all the photocaged tyrosine variants completely abrogated FLP activity when inserted in place of Y343. Likewise, we saw no Citrine2 expression in animals grown without ncAA (**Supplementary Fig. 2**).

Photocaging FLP at Lysine 223

To photocage FLP at the catalytic lysine K223, we tested two different photocaged lysine variants. The photocaged lysine variants 6-nitropiperonyl-L-Lysine (PCK) and hydroxycoumarin-lysine (HCK) have previously been used to photocage Cre activity by us and others[10–12]. We have previously demonstrated the efficient incorporation of PCK in *C. elegans* using the evolved PylRS variant PCKRS[12,27]. HCK on the other hand has not previously been established for use in *C. elegans*. We nevertheless wanted to explore its suitability for photocaging FLP activity, since HCK has been reported to display efficient uncaging at longer wavelength[28].

We first tested whether HCK can be incorporated into proteins in *C. elegans* by constructing strains ubiquitously expressing HCKRS, a PylRS variant evolved for incorporating HCK[28], together with tRNA(M15)$_{CUA}$ and a fluorescent GFP::mCherry reporter containing an amber stop codon between the GFP and mCherry reading frames (**Supplementary Fig. 1a**)[29]. We found that HCK can indeed be incorporated in *C. elegans* efficiently by HCKRS, comparable in efficiency to PCK incorporation using PCKRS (**Supplementary Fig. 1b**).

Interestingly, when we tested cross-reactivity of PCKRS and HCKRS with the two lysine variants, we found that HCKRS efficiently recognized PCK, resulting in incorporation levels comparable to those observed with HCK (**Supplementary Fig. 1b**). In contrast, although PCKRS was capable of incorporating HCK, its efficiency only reached 50% compared to that achieved with PCK. Notably, in strains expressing HCKRS we observed low but clearly detectable production of full length GFP::mCherry protein even in the absence of either ncAA, indicating non-specific amber stop codon read-through in our system and potential incorporation of a canonical amino acid. By comparison, no such full-length reporter protein was detected in strains expressing PCKRS grown in the absence of ncAA. We therefore explored whether we could improve the efficiency of PCKRS so it can be used for incorporation of both photocaged lysine variants PCK and HCK.

To improve efficiency of PCKRS, we tested mutations recently developed for the *M. mazei* PylRS using directed evolution that significantly increase the activity of the enzyme, but do not affect its ncAA specificity[30]. We introduced these mutations to PCKRS to create PCKRS(13IPYER), and found that PCKRS(13IPYER), while it did not show a significant improvement for incorporation of PCK, doubled incorporation levels for HCK (**Supplementary Fig. 1b**). Importantly, PCKRS(13IPYER) retained its fidelity in the absence of ncAA and did not result in production of full length GFP::mCherry without ncAA. We therefore used PCKRS(13IPYER) for further experiments involving either PCK or HCK.

We then generated transgenic *C. elegans* strains expressing PCKRS(13IPYER) together with tRNA(M15)$_{CUA}$, the FLP construct containing an amber stop codon at position K223, and the fluorescent Citrine2 reporter as described above.

To assay activation of PC-FLP using photocaged lysines, transgenic animals were grown from the L1 larval stage for 24 hours on NGM agar plates containing either 1 mM PCK or HCK followed by illumination with 365 nm light to remove the caging group and thus activate FLP. 24 hours after illumination we observed strong Citrine2 fluorescence in animals grown on either PCK or HCK (**Fig. 2c**). We observed activation efficiencies 83.8% and 77.4% when FLP was photocaged by PCK and HCK respectively using PCKRS(13IPYER) (**Fig.**

3a). In contrast activation efficiencies of 31.4% and 71.2% were observed when the HCKRS was used to incorporate PCK and HCK respectively (**Supplementary Fig. 1c**). We saw no Citrine2 expression in any animals grown on either PCK or HCK but not illuminated, indicating that both PCK and HCK were able to completely abrogate FLP activity when inserted in place of K223. Likewise, we saw no Citrine2 expression in animals grown without ncAA (**Supplementary Fig. 2**).

Photocaging FLP at Cysteine 189

To photocage FLP at C189 we generated transgenic *C. elegans* strains expressing PCC2RS, a PylRS variant evolved to recognise the photocaged cysteine PCC2[21], tRNA(M15)$_{CUA}$, FLP containing an amber stop codon at position C189, and the Citrine2 reporter to visualise activity of the recombinase.

To assay activity of PC-FLP caged using PCC2, transgenic animals were grown from the L1 larval stage for 24 hours on NGM agar plates containing 1 mM PCC2 followed by illumination with 365 nm light to remove the caging group and thus activate FLP. 24 hours after illumination we observed strong Citrine2 fluorescence in animals grown on PCC2 (**Fig. 2c**), corresponding to an activation efficiency of 83.6% (**Fig. 3a**). No Citrine2 fluorescence was observed in animals grown on PCC2 but not exposed to UV light or in animals grown without ncAA.

PC-FLP significantly outperforms PC-Cre in *C. elegans*

We next compared the efficiency of our PC-FLP system to the previously published PC-Cre variants photocaged at the catalytic residues K201 and Y324[9–12], which correspond to FLP K223 and Y343 respectively.

For a direct comparison, we created transgenic strains equivalent to the PC-FLP strains described above, but expressing PC-Cre. These strains contained the same PylRS/tRNA(M15)$_{CUA}$ variant pairs that we previously used to express PC-FLP, albeit together with Cre variants containing an amber stop codon at K201 or Y324, and a fluorescent reporter with loxP sites flanking the transcriptional stop cassette in place of FRT sites.

Animals expressing each of the systems were grown on their respective ncAAs for 24 hours from the L1 larval stage: the tyrosines ONBY, NPY and MNPY, and the lysines PCK and HCK. PC-FLP(C189PCC2) was also included in the assay even though no corresponding cysteine residue exists in Cre. The worms were then illuminated with 365 nm light and Citrine2 expression measured 24 hours later.

We found that for all ncAAs, PC-FLP significantly outperformed PC-Cre. For the photocaged lysines, we measured activation efficiencies in glutamatergic neurons of 83.8% and 77.4% for PC-FLP(K223PCK) and PC-FLP(K223HCK) respectively, compared to 62.3% for PC-Cre(K201PCK) and 56.6% for PC-Cre(K201HCK). Strikingly, all three PC-FLP variants utilising photocaged tyrosine variants, Y343NPY, Y343ONBY and Y343MNPY, showed high efficiencies of 99.1% 99.5% and 98.5% respectively, whereas PC-Cre(Y324NPY), PC-Cre(Y324ONBY), and PC-Cre(Y324MNPY) only yielded efficiencies of 68.9%, 39.2% and 52.4% respectively. PC-FLP(C189PCC2) also out-performed all PC-Cre variants with an efficiency 83.6% (**Fig. 3a**).

The differences became even more striking when we looked at efficiencies at lower ncAA concentrations and reduced the time on ncAA. For these experiments we focused only on the three photocaged tyrosines, which all showed close to 100% activity at 1 mM and 24 hours on ncAA when incorporated in place of Y343 in FLP. When we reduced ncAA concentrations, the best performing PC-FLP variant, PC-FLP(Y343NPY), showed 100% activity down to 0.01 mM, and 92.5% activity at 0.001 mM. PC-FLP(Y343ONBY) showed 89.3% activity at 0.01 mM and 20.2% at 0.001 mM. In contrast, the best performing PC-Cre(Y324NPY) showed only 2% at 0.01 mM and no detectable activity at 0.001 mM (**Fig. 3b**).

When we reduced the time on ncAA to 8 hours before illumination, thereby reducing the time window for production of PC-FLP and PC-Cre, all three PC-FLP(Y343) variants still showed between 95% to 100% activity at 1 mM, while the activity for all three PC-Cre(Y324) variants was reduced to below 20%. When we reduced the ncAA concentration 100-fold to 0.01 mM, PC-FLP(Y343NPY) animals still showed near 100% activation efficiency and PC-FLP(Y343ONBY) animals showed 82% activation efficiency. In contrast, no PC-Cre animals showed any detectable activity below 0.1 mM (**Fig. 3b**).

PC-FLP can be used to control expression of target genes with high efficiency and no background

Besides the fluorescent Citrine2 reporter, we also created *C. elegans* lines expressing the different PC-FLP variants in glutamatergic head neurons using the *glr-1p* promoter to control the expression of a Chrimson::F2A::Citrine2 construct that was separated from its promoter by a transcriptional terminator flanked by two FRT sites. When Chrimson is expressed in the glutamatergic head neurons of *C. elegans*, optogenetic activation leads to easily scorable reversals and accelerations[31]. We have previously used PC-Cre to control expression of the optogenetic channels ChR2 and Chrimson in these *C. elegans* neurons, allowing us to control neuronal activity and behaviour[12].

We grew transgenic animals expressing the PC-FLP systems on 1 mM of the corresponding photocaged ncAA for 48 hours from the L1 larval stage. We illuminated the animals with 365 nm light and then transferred them to NGM agar plates supplemented with all-trans retinal (ATR) for 24 hours to give time for expression of the functional Chrimson channel. We then performed optogenetic behavioural assays by illuminating the animals for 1 second using a 617 nm LED to activate Chrimson. Activity was scored by determining the fraction of animals responding to the stimulus.

In animals expressing PC-FLP, photocaged with either the photocaged lysine PCK or the photocaged tyrosines NPY, ONBY, MNPY, we found that 100% of animals responded to the stimulus. In the strains expressing FLP photocaged with PCC2, 90% of animals responded to the stimulus (**Fig. 3c**). Importantly, we saw no response in animals grown on any of the ncAAs, but not illuminated, further confirming that all photocaged ncAAs fully block the function of FLP and allow tight control of target gene expression.

PC-FLP is functional in tissues outside the nervous system

We next wanted to determine whether PC-FLP could be generally applied in tissues other than the nervous system. For this, we generated strains to express the best performing PC-FLP variant, PC-FLP(Y343NPY), in either the pharynx, or body wall muscle cells. The synthetase NPYRS and FLP were driven by the *myo-2p* promoter for expression in the pharynx, or the *myo-3p* promoter for expression in body wall muscle cells. In both cases we used the ubiquitous *eef-1A.1p* (*eft-3p)* promoter to drive expression of the Citrine2 reporter gene.

Transgenic animals were grown from the L1 larval stage for 48 hours on NGM agar plates containing 1 mM NPY to express PC-FLP(Y343NPY), followed by illumination at 365 nm. 24 hours after illumination worms were assayed for Citrine2 fluorescence. In both cases for animals expressing PC-FLP(Y343NPY) in either the pharynx or the body wall muscle, we observed clearly visible Citrine2 fluorescence. In contrast, we observed no fluorescence in animals grown on 1 mM NPY but not illuminated (**Fig. 4a**).

To further compare FLP to Cre, we also generated strains expressing the corresponding PC-Cre(Y324NPY) in the pharynx and in body wall muscle. Here, in contrast to PC-FLP(Y343NPY), we found no strains that displayed more than very weak Citrine2 expression in few cells for both tissues, again showing that PC-FLP is significantly more efficient than PC-Cre (**Fig. 4a, Supplementary Fig. 3**).

PC-FLP can be efficiently activated with wavelengths longer than 365 nm

One of the main advantages of controlling the activity of SSRs using photocaged ncAAs is the speed of the uncaging reaction allowing for the permanent activation of the SSR using a very brief pulse of light in the low second or even sub-second range. This light can be targeted very precisely to localise the activation to single cells in living animals[12]. We have previously carried out single-cell activation of PC-Cre using a microscope-mounted laser to deliver 365 nm light. While the photocaging groups used here are most sensitive to wavelengths below 400 nm, we nevertheless wanted to test activation efficiencies at longer wavelengths, since it would be highly advantageous to be able to efficiently activate PC-FLP at a wavelength of 405 nm so that single cell activation could be carried out using a standard 405 nm laser commonly used on confocal microscopes.

When we recorded the absorption spectra of the photocaged ncAAs used here, we found that, encouragingly, all ncAAs absorbed at 405 nm, albeit with ONBY showing lower absorption than the other compounds (**Supplementary Fig. 4a**).

We first assayed the activation of PC-FLP at different wavelength ranges using LED illumination. For this, animals expressing the PC-FLP systems were grown from the L1 larval stage for 24 hours on NGM agar

plates containing their respective ncAA at a concentration of 1 mM. The worms were then illuminated for 5 minutes using LEDs to deliver light with peak wavelengths of 365 nm, 405 nm, 435 nm, 460 nm, or 470 nm (**Supplementary Fig. 4b**). In all cases, we found that PC-FLP variants activated efficiently at 365 nm, and that there was no significant difference between the activation efficiency with the 365 nm LED and 405 nm LED. With the 435 nm LED, we observed none or only marginal activation of PC-FLP in animals expressing PC-FLP(K223PCK), PC-FLP(K223HCK), and PC-FLP(Y343ONBY), while animals expressing PC-FLP(Y343NPY) showed an activation efficiency of 6%. In contrast, animals expressing PC-FLP(Y343MNPY) or PC-FLP(C189PCC2) both showed efficient activation of 55% and 68.8% respectively (**Fig. 5a**).

Importantly, we further tested the stability of the PCC2 and MNPY photocages at wavelengths above 435 nm and found that there was only negligible activation of approximately 1% for PC-FLP(C189PCC2) with the 460 nm LED, and no activation with the 470 nm LED. PC-FLP(Y343MNPY) was not activated by either 460 nm or 47 nm LED illumination. Furthermore, we observed no activation after illuminating using a standard 480/20 nm GFP filter for 5 minutes or exposing animals expressing PC-FLP(C189PCC2) to standard laboratory ambient lighting for 24 hours, demonstrating that PC-FLP(C189PCC2) and PC-FLP(Y343MNPY) are still compatible with blue-light optogenetics and imaging (**Supplementary Fig. 4c**).

Activation of PC-FLP using a 405 nm microscope mounted laser

We then proceeded to test activation of the different PC-FLP variants using a standard confocal 405 nm laser. For this, animals were again grown from the L1 larval stage for 48 hours on NGM agar plates containing their respective ncAA at a concentration of 1 mM. They were then anaesthetized, mounted on agar slides, and we scanned their head region using the 405 nm laser at various power settings. The animals were then recovered onto NGM agar plates and imaged to quantify activation efficiency 24 hours after illumination. We found that at 50% laser power, PC-FLP(Y343NPY), PC-FLP(Y343MNPY), and surprisingly even PC-FLP(Y343ONBY) were activated with near 100% efficiency. At 10% laser power, PC-FLP(Y343NPY) was still activated with 100% efficiency, and PC-FLP(Y343MNPY) with 84.3% efficiency, but we saw no activation of PC-FLP(Y343ONBY). At 1% laser power we only saw activation of PC-FLP(Y343MNPY) at 8.3% efficiency. For the PC-FLP variants containing the photocaged lysines, PC-FLP(K223PCK) and PC-FLP(K223HCK), at 50% laser power we observed activation efficiencies of 33.4% and 21.4% respectively. At 10% laser power we saw only minimal activation of PC-FLP(K223PCK) (1.9%), and no activity for PC-FLP(K223HCK). Interestingly, PC-FLP(C189PCC2) never displayed activity above 64.5%, but showed similar activation efficiencies at all three power levels of 50%, 10% and 1% respectively (**Fig. 5b and Supplementary Fig. 4d**)

Having confirmed that several PC-FLP variants can be efficiently activated using a 405 nm laser at a range of power levels, we next tested whether the confocal microscope would serve to precisely target PC-FLP activation to single cells. We carried out this experiment with the PC-FLP(Y343NPY) animals at 10% laser power and targeted the bilaterally symmetric PVC neurons in the tail, since the *glr-1p* promoter used to drive FLP and NPYRS is active in these neurons.

Worms were grown from the L1 larval stage for 48 hours on NGM agar plates containing 1 mM NPY. They were then anaesthetized and mounted on agar slides. We then targeted the laser to one of the PVCs using the bleaching function to illuminate in a single Z-stack. 24 hours after illumination we observed Citrine2 only in the cell that was targeted by the laser (**Fig. 5c**)

DISCUSSION

We develop a photoactivatable FLP recombinase by incorporating photocaged non-canonical amino acids into FLP using genetic code expansion technology. We demonstrate that the activity of FLP can be photocaged by replacing any one of the active site residues Tyr343, Lys223, and Cys189 with their respective photocaged counterpart. We find that in all cases, PC-FLP variants function more efficiently than PC-Cre and that in general, PC-FLP outperforms PC-Cre under all conditions and in all tissues we have tested.

We further establish that PC-FLP can be efficiently activated using light with wavelengths longer than 365 nm, thus allowing the use of a standard 405 nm microscope-mounted laser to activate the expression of target genes with single-cell precision. This makes PC-FLP easily accessible for most laboratories as a tool to control gene expression with single cell precision, without the need for specialised equipment.

Furthermore, the availability of two SSRs, photocageable using various photocaged ncAAs (Lys, Tyr, Cys) raises the exciting future possibility of combining PC-FLP and PC-Cre, photocaged by different ncAAs, to create even more powerful tools for optically controlling gene expression. Our finding that some of the photocaged ncAAs tested (MNPY, PCC2) can be efficiently uncaged at longer wavelengths, while others show no uncaging at these wavelengths (PCK, HCK) suggests the prospect of differentially activating PC-FLP and PC-Cre using different wavelengths of light.

The use of two photocaged ncAAs would however require mutually orthogonal PylRS/tRNA pairs for the incorporation of one photocaged ncAA into FLP and a different photocaged ncAA into Cre in the same cell. While several such mutually orthogonal PylRS/tRNA(Pyl) pairs have been established in *E. coli* and mammalian cell culture systems[32–35], none have thus far been reported for multicellular organisms. Additionally, apart from the PylRSs from *Methanosarcina* species, which are not mutually orthogonal, no PylRSs are available for incorporation of photocaged ncAAs. It is however foreseeable that these limitations will be overcome in the near future.

The fact that FLP activity can be precisely controlled through the incorporation of photocaged ncAAs suggests the possibility that this approach will be transferrable to other SSRs beside FLP and Cre. Several other tyrosine SSRs related to FLP and Cre, such as Dre, Vika, B3, KD, have been established in a variety of different models[2]. Given the high sequence homology to some members and conserved mechanism of action, it is not unlikely likely these too could be photocaged using the straightforward replacement of critical amino acid residues with photocaged variants as outlined here.

While this work has been carried out in *C. elegans*, the components it uses are not specific to worms and we expect them to be transferable to other systems in which FLP and genetic code expansion have been established, including bacteria, cultured mammalian cells and organoids, as well as other animal models such zebrafish, *Drosophila*, and mouse.

METHODS

C. elegans strains

Strains were maintained under standard conditions unless otherwise indicated[36,37]. Transgenic strains were generated by biolistic bombardment using hygromycin B as a selection marker[29,38,39]. Strains were maintained on Nematode growth medium (NGM) supplemented with hygromycin at a concentration of 0.3 mg/ml (Formedium).

ncAA feeding

PCK[27] was custom synthesised by ChiroBlock GmbH, Germany. HCK[28] was custom synthesised by Inochem, United Kingdom. NPY[25] was custom synthesised by NewChem Technologies, UK. MNPY[25] was custom synthesised by NewChem Technologies, UK. ONBY[40] was purchased from Fluorochem. PCC2[21] was custom synthesised by ChiroBlock GmbH, Germany. NGM plates containing ncAA (ncAA-NGM) were prepared by dissolving the ncAA in a small volume of HCl or NaOH and then adding it to the molten NGM. The HCl or NaOH were then neutralised by equimolar NaOH or HCl respectively. PCK was dissolved in 0.2 M HCl, HCK was dissolved in 0.1 M NaOH, NPY was dissolved in 1 M NaOH, MNPY was dissolved in 0.1 M NaOH, ONBY was dissolved in 1 M NaOH, PCC2 was dissolved in 0.5 M HCl.

Animals were age-synchronised by settling and added to ncAA-NGM plates as L1 larvae. Freeze-dried OP50 (LabTIE) reconstituted according to the manufacturer's instructions was added for food. Animals were grown on the ncAA-NGM plates for 24 hours unless otherwise stated.

Photocaged Recombinase activation

For global activation, worms were washed off NGM plates with M9 supplemented with 0.001% Triton-X100. To test activation, animals were illuminated in a CL-1000L crosslinker at 365 nm (Analytik Jena) for 5 minutes. To test activation at defined longer wavelengths, a pE-4000 light source (CoolLED) was used. Worms were illuminated with the "365 nm", "405 nm", "435 nm", "460 nm", or "470 nm" LEDs at 100% power for 5 minutes. These LEDs produce light in the following ranges: "365 nm" (350 nm to 415 nm), "405 nm" (370 nm to 443 nm), "435 nm" (403 nm to 470 nm), "460 nm" (427 to 510 nm) and "470 nm" (433 nm to 522 nm) (see also **Supplementary Fig 4b**).

For laser activation at 405 nm, a Zeiss LSM800 laser scanning confocal microscope was used. Worms were anaesthetized with 50 mM NaN3 and mounted on 2.5% agar pads on microscope slides. For whole-head illumination, the worms were located with the 20x objective, and the bleaching function was run for 10 iterations with a 2.31 µs dwell time at 2 µm Z-stack intervals across the entire width of the worm. For single-cell illumination, worms were located with the 20x objective and a 6x area crop was applied. The bleaching function was run for 20 iterations with a 2.31 µs dwell time at a single Z-plane within a 'Region of Interest' that was drawn around the cell body of the target neuron.

Imaging and analysis

All imaging was carried out on a Zeiss Axio Imager M2. Worms were anaesthetized with 50 mM NaN_3 and mounted on 2.5% agar pads on microscope slides. All image analysis was carried out on Fiji version 2.14.0. To score activation efficiency, the area in which the fluorescent Citrine2 reporter was expressed was compared to the area in which the fluorescent mKate2 marker was expressed. To do this, the fluorescent mKate2 marker within worms was first automatically identified using Li thresholding. This thresholding was used to create a mask that was applied onto the fluorescent Citrine2 reporter channel. Within this mask the number of pixels that exceeded the signal threshold were counted as signal. The activation efficiency was calculated as the ratio of signal pixels to mask pixels, expressed as a percentage. Statistical analysis was carried out using GraphPad Prism version 10. The fluorescence images shown in the figures were taken using an Apotome 3 module mounted on the Zeiss Axio Imager M2. Images for quantification were taken without the Apotome 3 module.

Behavioural assays

Worms were grown on ncAA-NGM plates for 48 hours. They were then illuminated with 365 nm light for 5 minutes or kept in the dark, after which they were transferred to plates seeded with 20uL of 0.35 OD *E. coli* OP50 supplemented with ATR to a concentration of 100 µM. Worms were grown in the presence of ATR for 24 hours. Behavioural assays were then carried out on a WormLab setup (MBF Bioscience). Animals were illuminated using the integrated 617 nm LED at 5 W/cm² for 1 second. Responses were scored manually from the recorded movies.

Recording of ncAA spectra

To measure the UV-Vis spectra of the photocaged ncAAs, they were firstly dissolved in HCl or NaOH as described above. The dissolved ncAA was then added to 25mM potassium phosphate buffer (pH6) to a final concentration of 0.5 mM. UV-Vis spectra were recorded on a Nanodrop 2000 (Thermo Fisher Scientific).

ACKNOWLEDGEMENTS
We thank Maria Doitsidou, Deep Prakash and Rebekah White for helpful suggestions on the manuscript. We thank the staff at the IMPACT imaging facility at the University of Edinburgh for assistance in the initial setup of laser uncaging experiments.

AUTHOR CONTRIBUTIONS
S.G. conceived of the project, J.J.V.R and S.G. designed experiments, J.J.V.R performed experiments and analysed data, K.B. performed initial experiments, J.J.V.R and S.G wrote the manuscript.

FUNDING
The work was supported by the European Research Council [ERC-StG-679990], the BBSRC [BB/Y006380/1 & BB/W014610/1], The Royal Society, The Muir Maxwell Epilepsy Centre.

REFERENCES

1. Fischer, J. A., Giniger, E., Maniatis, T. & Ptashne, M. GAL4 activates transcription in Drosophila. *Nature* **332**, 853–856 (1988).
2. Meinke, G., Bohm, A., Hauber, J., Pisabarro, M. T. & Buchholz, F. Cre Recombinase and Other Tyrosine Recombinases. *Chem. Rev.* **116**, 12785–12820 (2016).
3. Feil, R. *et al.* Ligand-activated site-specific recombination in mice. *Proc. Natl. Acad. Sci.* **93**, 10887–10890 (1996).
4. Muñoz-Jiménez, C. *et al.* An Efficient FLP-Based Toolkit for Spatiotemporal Control of Gene Expression in *Caenorhabditis elegans*. *Genetics* **206**, 1763–1778 (2017).
5. Schmitt, C., Schultheis, C., Husson, S. J., Liewald, J. F. & Gottschalk, A. Specific Expression of Channelrhodopsin-2 in Single Neurons of Caenorhabditis elegans. *PLoS ONE* **7**, e43164 (2012).
6. Jung, H. *et al.* Noninvasive optical activation of Flp recombinase for genetic manipulation in deep mouse brain regions. *Nat. Commun.* **10**, 314 (2019).
7. Schindler, S. E. *et al.* Photo-activatable Cre recombinase regulates gene expression in vivo. *Sci. Rep.* **5**, 13627 (2015).
8. Charette, M., Rosenblum, C., Shade, O. & Deiters, A. Optogenetics with Atomic Precision—A Comprehensive Review of Optical Control of Protein Function through Genetic Code Expansion. *Chem. Rev.* **125**, 1663–1717 (2025).
9. Edwards, W. F., Young, D. D. & Deiters, A. Light-Activated Cre Recombinase as a Tool for the Spatial and Temporal Control of Gene Function in Mammalian Cells. *ACS Chem. Biol.* **4**, 441–445 (2009).
10. Luo, J. *et al.* Genetically encoded optical activation of DNA recombination in human cells. *Chem. Commun.* **52**, 8529–8532 (2016).
11. Brown, W., Liu, J., Tsang, M. & Deiters, A. Cell-Lineage Tracing in Zebrafish Embryos with an Expanded Genetic Code. *ChemBioChem* **19**, 1244–1249 (2018).
12. Davis, L. *et al.* Precise optical control of gene expression in C. elegans using improved genetic code expansion and cre recombinase. *eLife* **10**, 1–22 (2021).
13. Broach, J. R. & Hicks, J. B. Replication and Recombination Functions Associated with the Yeast Plasmid, 2μ Circle. *Cell* **21**, 501–508 (1980).
14. Buchholz, F. Different thermostabilities of FLP and Cre recombinases: implications for applied site-specific recombination. *Nucleic Acids Res.* **24**, 4256–4262 (1996).
15. Buchholz, F., Angrand, P.-O. & Stewart, A. F. Improved properties of FLP recon1binase evolved by cycling n1utagenesis. **16**, (1998).

16. Heidmann, D. & Lehner, C. F. Reduction of Cre recombinase toxicity in proliferating Drosophila cells by estrogen-dependent activity regulation. *Dev. Genes Evol.* **211**, 458–465 (2001).
17. Nern, A., Pfeiffer, B. D., Svoboda, K. & Rubin, G. M. Multiple new site-specific recombinases for use in manipulating animal genomes. *Proc. Natl. Acad. Sci.* **108**, 14198–14203 (2011).
18. Crnković, A., Suzuki, T., Söll, D. & Reynolds, N. M. Pyrrolysyl-tRNA Synthetase, an Aminoacyl-tRNA Synthetase for Genetic Code Expansion. *Croat. Chem. Acta* **89**, (2016).
19. Nunes-Duby, S. E., Kwon, H. J., Tirumalai, R. S., Ellenberger, T. & Landy, A. Similarities and differences among 105 members of the Int family of site-specific recombinases. *Nucleic Acids Res.* **26**, 391–406 (1998).
20. Chen, J.-W., Evans, B. R., Yang, S.-H., Araki, H. & Jayaram, M. Functional Analysis of Box I Mutations in Yeast Site-Specific Recombinases Flp and R: Pairwise Complementation with Recombinase Variants Lacking the Active-Site Tyrosine. *MOL CELL BIOL* **12**, (1992).
21. Nguyen, D. P. *et al.* Genetic Encoding of Photocaged Cysteine Allows Photoactivation of TEV Protease in Live Mammalian Cells. *J. Am. Chem. Soc.* **136**, 2240–2243 (2014).
22. Xi, Z. *et al.* Using a quadruplet codon to expand the genetic code of an animal. *Nucleic Acids Res.* **50**, 4801–4812 (2022).
23. Nikić, I. *et al.* Debugging Eukaryotic Genetic Code Expansion for Site-Specific Click-PAINT Super-Resolution Microscopy. *Angew. Chem. Int. Ed.* **55**, 16172–16176 (2016).
24. Serfling, R. *et al.* Designer tRNAs for efficient incorporation of non-canonical amino acids by the pyrrolysine system in mammalian cells. *Nucleic Acids Res.* **46**, 1–10 (2018).
25. Luo, J., Torres-Kolbus, J., Liu, J. & Deiters, A. Genetic Encoding of Photocaged Tyrosines with Improved Light-Activation Properties for the Optical Control of Protease Function. *ChemBioChem* **18**, 1442–1447 (2017).
26. O'Shea, J. M. *et al.* Generation of Photocaged Nanobodies for Intracellular Applications in an Animal Using Genetic Code Expansion and Computationally Guided Protein Engineering**. *ChemBioChem* **23**, e202200321 (2022).
27. Gautier, A. *et al.* Genetically Encoded Photocontrol of Protein Localization in Mammalian Cells. *J. Am. Chem. Soc.* **132**, 4086–4088 (2010).
28. Luo, J. *et al.* Genetically encoded optochemical probes for simultaneous fluorescence reporting and light activation of protein function with two-photon excitation. *J. Am. Chem. Soc.* **136**, 15551–15558 (2014).
29. Greiss, S. & Chin, J. W. Expanding the Genetic Code of an Animal. *J. Am. Chem. Soc.* **133**, 14196–14199 (2011).

30. Tseng, H.-W. *et al.* Expanding the Scope of Orthogonal Translation with Pyrrolysyl-tRNA Synthetases Dedicated to Aromatic Amino Acids. *Molecules* **25**, 4418 (2020).
31. Stirman, J. N. *et al.* Real-time multimodal optical control of neurons and muscles in freely behaving Caenorhabditis elegans. *Nat. Methods* **8**, 153–158 (2011).
32. Willis, J. C. W. & Chin, J. W. Mutually orthogonal pyrrolysyl-tRNA synthetase/tRNA pairs. *Nat. Chem.* **10**, 831–837 (2018).
33. Beránek, V., Willis, J. C. W. & Chin, J. W. An Evolved *Methanomethylophilus alvus* Pyrrolysyl-tRNA Synthetase/tRNA Pair Is Highly Active and Orthogonal in Mammalian Cells. *Biochemistry* **58**, 387–390 (2019).
34. Meineke, B., Heimgärtner, J., Lafranchi, L. & Elsässer, S. J. *Methanomethylophilus alvus Mx1201* Provides Basis for Mutual Orthogonal Pyrrolysyl tRNA/Aminoacyl-tRNA Synthetase Pairs in Mammalian Cells. *ACS Chem. Biol.* **13**, 3087–3096 (2018).
35. Meineke, B., Heimgärtner, J., Eirich, J., Landreh, M. & Elsässer, S. J. Site-Specific Incorporation of Two ncAAs for Two-Color Bioorthogonal Labeling and Crosslinking of Proteins on Live Mammalian Cells. *Cell Rep.* **31**, 107811 (2020).
36. Brenner, S. THE GENETICS OF CAENORHABDITIS ELEGANS. *Genetics* **77**, 71–94 (1974).
37. Stiernagle, T. Maintenance of C. elegans. *WormBook* (2006) doi:10.1895/wormbook.1.101.1.
38. Davis, L. & Greiss, S. Genetic Encoding of Unnatural Amino Acids in C. elegans. in *Noncanonical Amino Acids* (ed. Lemke, E. A.) vol. 1728 389–408 (Springer New York, New York, NY, 2018).
39. Radman, I., Greiss, S. & Chin, J. W. Efficient and Rapid C. elegans Transgenesis by Bombardment and Hygromycin B Selection. *PLoS ONE* **8**, e76019 (2013).
40. Deiters, A., Groff, D., Ryu, Y., Xie, J. & Schultz, P. G. A Genetically Encoded Photocaged Tyrosine. *Angew. Chem. Int. Ed.* **45**, 2728–2731 (2006).
41. Chen, Y. Crystal Structure of a Flp Recombinase–Holliday Junction Complex Assembly of an Active Oligomer by Helix Swapping. *Mol. Cell* **6**, 885–897 (2000).

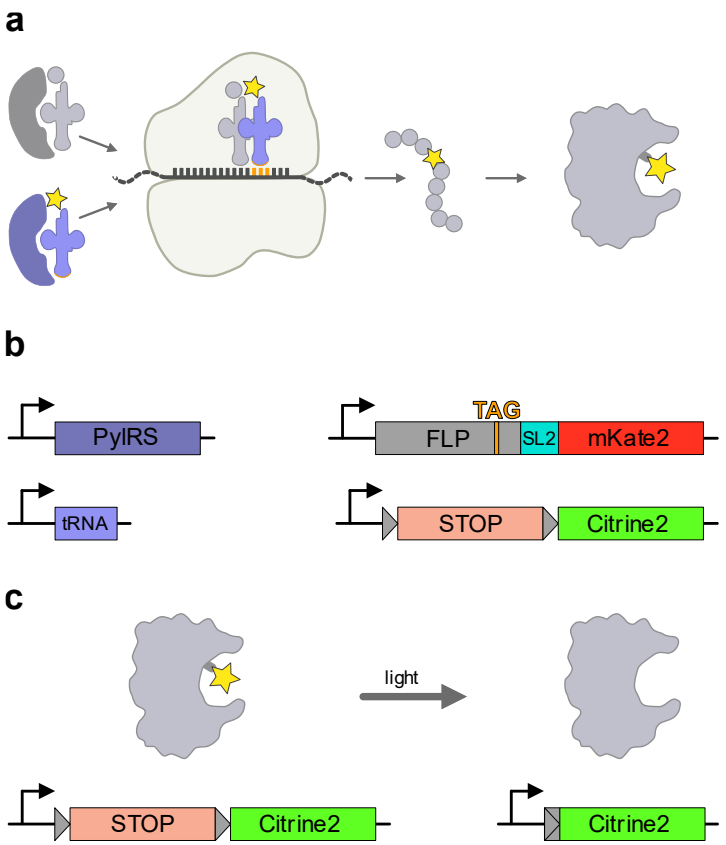

Fig. 1 Photocaging the activity of FLP recombinase using genetic code expansion. a The orthogonal PylRS aminoacylates its cognate orthogonal tRNA (blue pair) with the ncAA (yellow star). The amino-acylated orthogonal tRNA then directs the incorporation of the ncAA into the growing polypeptide chain in response to the amber stop codon. This results in the incorporation of the photocaged ncAA into FLP to produce PC-FLP. **b** Constructs transformed into *C. elegans* for expression and visualisation of PC-FLP. The PylRS and tRNA serve to direct the incorporation of the various photocaged ncAAs into the FLP gene at the amber stop codon. The FLP is expressed in an operon with mKate2 to visualise its expression. The reporter is made up of a Citrine2 gene whose expression is prevented by an upstream transcriptional stop cassette that is flanked by FRT sites. **c** PC-FLP, which is photocaged by the incorporation of a photocaged ncAA into its active site is unable to excise the transcriptional stop cassette inserted between the Citrine2 reporter gene and its promoter. Following illumination, the photocaging group within the PC-FLP is removed, producing active FLP, which is able to excise the transcriptional terminator and allow for the production of Citrine2.

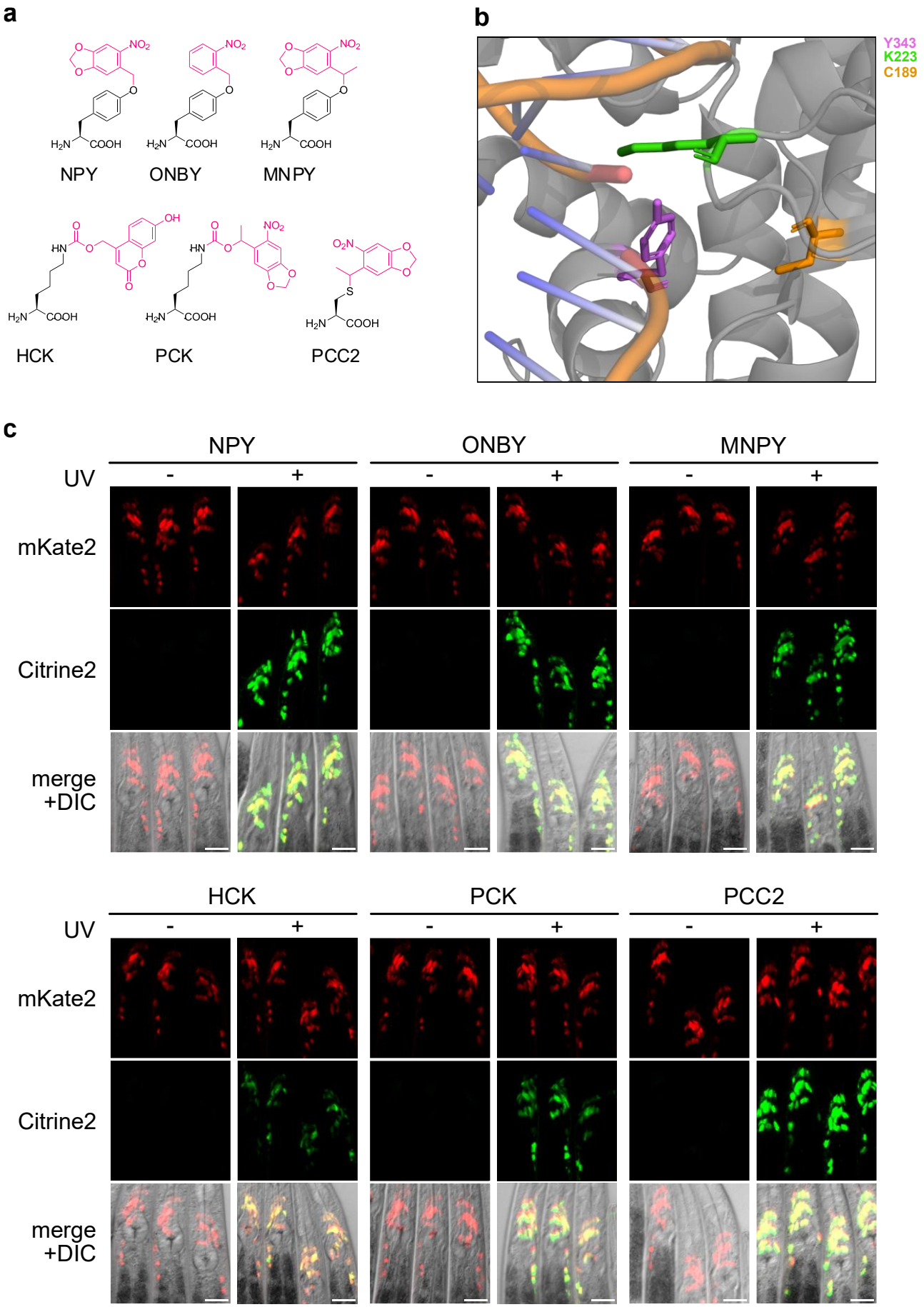
a
NPY
ONBY
MNPY
HCK
PCK
PCC2
b
Y343
K223
C189
c
NPY
ONBY
MNPY
UV
-
+
mKate2
Citrine2
merge
+DIC
HCK
PCK
PCC2

Fig. 2 PC-FLP system. a Chemical structures of photocaged ncAAs used in this paper. The photocaging groups are highlighted in pink. **b** Active site of FLP recombinase (PDB: 1FLO[41]) with active site residues Y343, K223, and C189 highlighted in purple, green, and orange respectively. **c** Fluorescence microscopy images of *C. elegans* head regions expressing the PC-FLP system using the different photocaged variants of tyrosine, lysine, and cysteine. Worms were grown in the presence of the respective ncAA at a concentration of 1 mM for 24 hours and then illuminated for 5 minutes with 365 nm ("+" condition) or kept in the dark ("-" condition). Scale bars represent 20 µm.

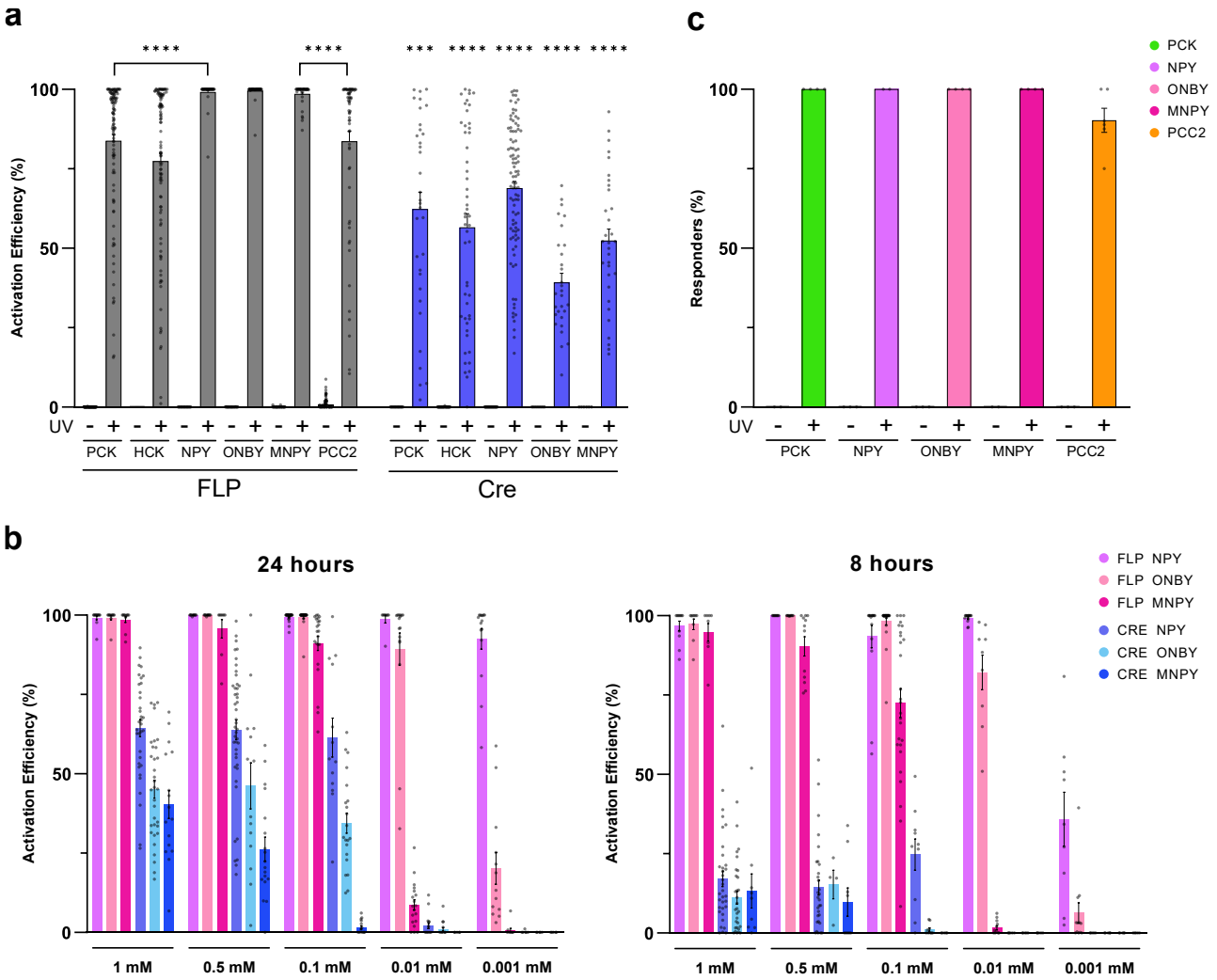

Fig. 3 Characterisation of PC-FLP and PC-Cre variants. a Activation efficiency in animals expressing PC-FLP and PC-Cre systems using photocaged variants of tyrosine, lysine, and cysteine. Animals were grown in the presence of the respective ncAA at a concentration of 1 mM for 24 hours and then illuminated with 365 nm light ("+" condition) or kept in the dark ("-" condition). Images were taken for quantification 24 hours after illumination. Dots represent individual animals assayed. Error bars represent the SEM. Significance values are determined by Welch's t-test. **b** Activation efficiency in animals expressing the PC-FLP and PC-Cre systems using the three photocaged tyrosine variants NPY, ONBY, and MNPY at decreasing concentrations. The panel on the left shows activation efficiency for worms exposed to the ncAAs for 24 hours. The panel on the right shows activation efficiency for worms exposed to the ncAAs for 8 hours. Dots represent individual animals assayed. Error bars represent the SEM. **c** PC-FLP was used to activate expression of the optogenetic channel Chrimson. Graphs show the percentage of animals expressing the PC-FLP system using the different photocaged variants of tyrosine, lysine, and cysteine that respond to a 1 second pulse of 5 W/cm^2 617 nm light 24h after FLP activation using 365 nm light. Worms were grown in the presence of the respective ncAA at a concentration of 1 mM for 48 hours and then illuminated with 365 nm ("+" condition) or kept in the dark ("-" condition). The worms were then transferred to plates supplemented with ATR and behavioural response assayed 24 hours later.

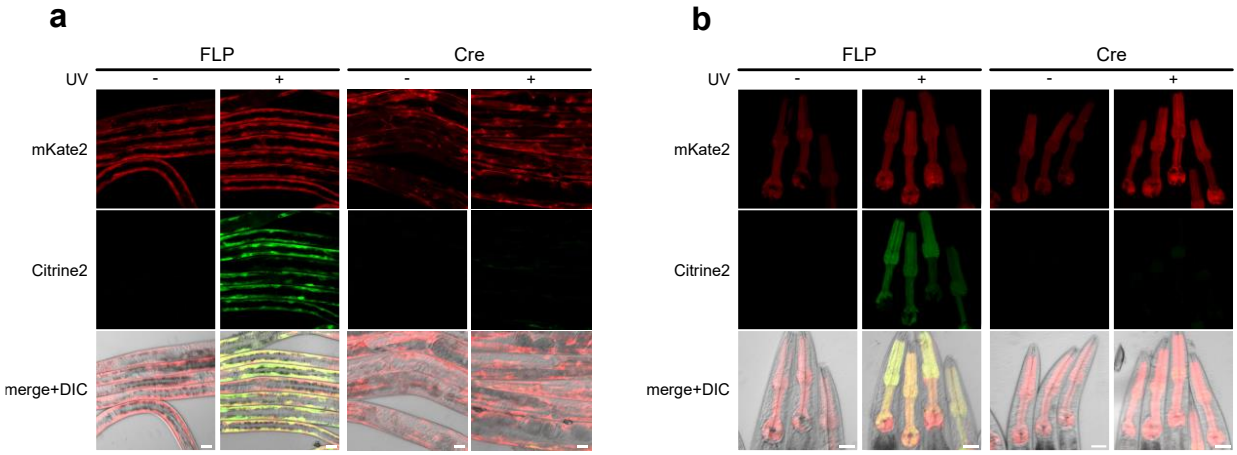

Fig. 4 PC-FLP and PC-Cre in the body wall muscle and the pharynx. a Fluorescence microscopy of worms expressing the PC-FLP and PC-Cre systems using the photocaged tyrosine NPY in the body wall muscle driven by the promoter for *myo-3*. Worms were grown in the presence of NPY at a concentration of 1 mM for 48 hours and then illuminated with 365 nm ("+" condition) or kept in the dark ("-" condition). Animals were imaged 24 hours after illumination. Scale bars represent: 20 µm. **b** Fluorescence microscopy of worms expressing the PC-FLP and PC-Cre systems using the photocaged tyrosine NPY in the pharynx driven by the promoter for *myo-2*. Worms were grown in the presence of NPY at a concentration of 1 mM for 48 hours and then illuminated with broad-band UV light ("+" condition) or kept in the dark ("-" condition). The worms were then imaged 24 hours after illumination. Scale bars represent: 20 µm.

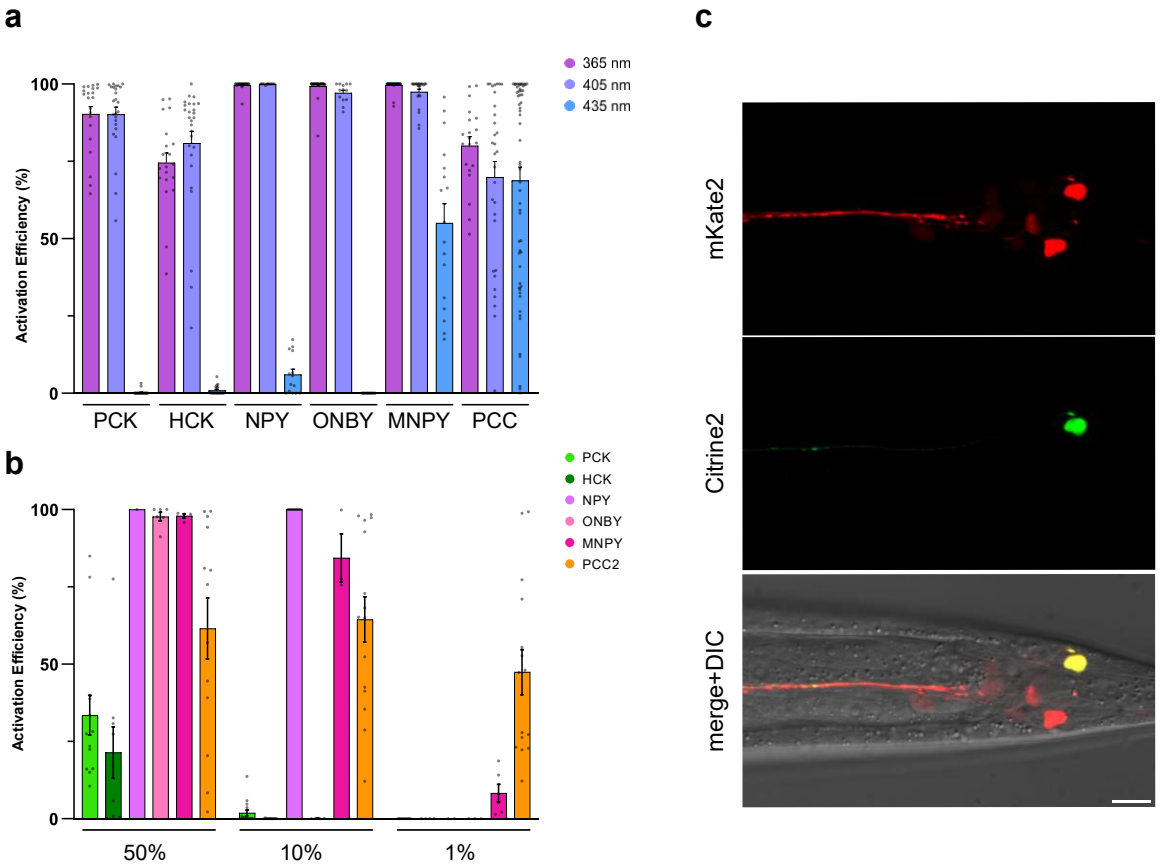

Fig. 5 Activation of PC-FLP variants at longer wavelengths. a Activation efficiency in animals expressing PC-FLP using the different photocaged variants of tyrosine, lysine, and cysteine following illumination using LEDs of various wavelengths. Worms were grown in the presence of the respective ncAA at a concentration of 1 mM for 24 hours and then illuminated for 5 minutes. The worms were then imaged for quantification 24 hours after illumination. Dots represent individual animals assayed. Error bars represent the SEM. **b**

Activation efficiency in animals expressing PC-FLP using the different photocaged variants of tyrosine, lysine, and cysteine following illumination with the 405 nm laser on the Zeiss LSM800 confocal microscope. Worms were grown in the presence of the respective ncAA at a concentration of 1 mM for 48 hours and then illuminated for 5 minutes. The worms were then imaged for quantification 24 hours after illumination. Percentage categories represent the pseudo-percentage laser power settings. Dots represent individual animals assayed. Error bars represent the SEM. **c** Fluorescence microscopy images showing expression of Citrine2 in a single PVC neuron 24 hours after targeted illumination with the 405 nm laser on the Zeiss LSM800. Scale bar represents: 10 µm.

Supplementary Information

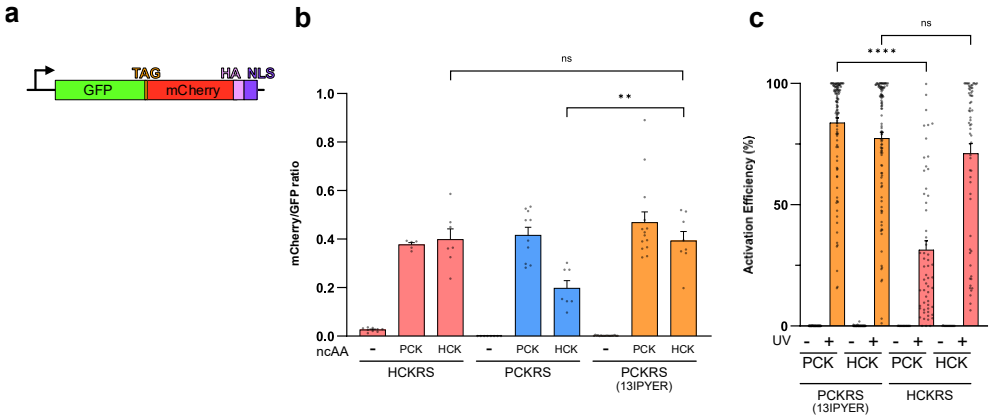

Supplementary Fig. 1 Comparison of HCKRS and PCKRS. a Schematic of GFP::mCherry construct used to quantify incorporation by the various PylRS variants. **b** mCherry/GFP ratio of animals expressing HCKRS, PCKRS, or PCKRS(13IPYER) grown for 24 hours on plates with no added ncAA (“-” condition), 1 mM of PCK, or 1 mM of HCK. Dots represent groups of animals assayed. Error bars represent the SEM. Significance values are determined by Welch's t-test. **c** Activation efficiency of animals expressing the HCKRS or PCKRS(13IPYER) to incorporate PCK or HCK into FLP recombinase. Worms were grown in the presence of the 1 mM PCK or 1 mM HCK for 24 hours and then illuminated for 5 minutes with 365 nm light ("+" condition) or kept in the dark ("-" condition). The worms were then imaged for quantification 24 hours after illumination. Dots represent individual animals assayed. Error bars represent the SEM. Significance values are determined by Welch's t-test.

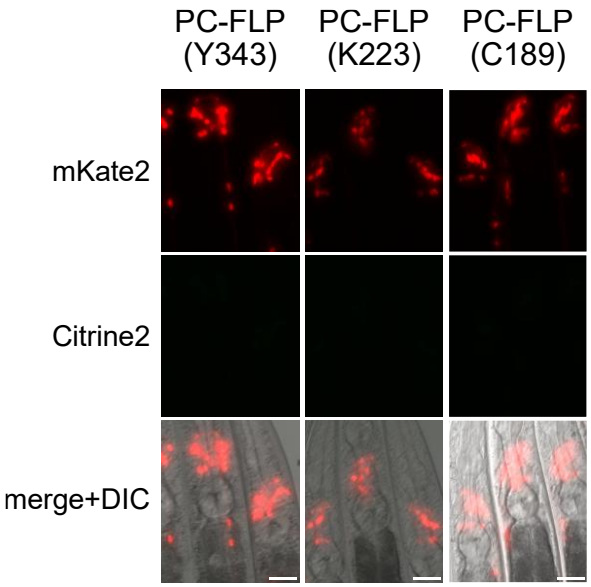

Supplementary Fig. 2 PC-FLP in the absence of ncAA. Fluorescence microscopy of worms expressing the PC-FLP(Y343), PC-FLP(K201), or PC-FLP(C189) system grown in the absence of ncAA. There is no expression of the Citrine2 reporter.

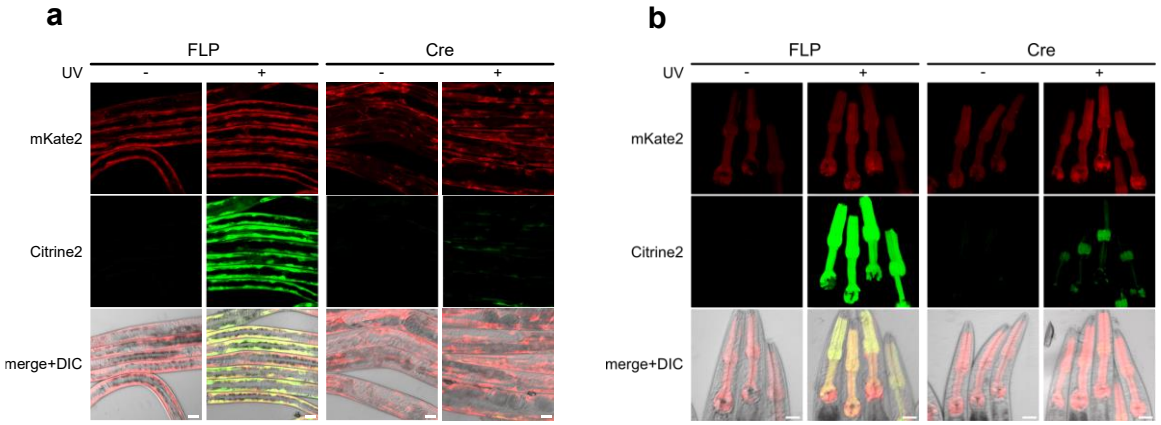

Supplementary Fig. 3 PC-FLP and PC-Cre in the body wall muscle and the pharynx. Fluorescence microscopy of worms expressing PC-FLP(Y343NPY) or PC-Cre(Y324NPY) in the body-wall or pharynx. Same set of images as in **Figure 4** but with brightness in the Citrine2 channel increased by **a** 100%, **b** 200% for clear visualization of inferior PC-Cre activity.

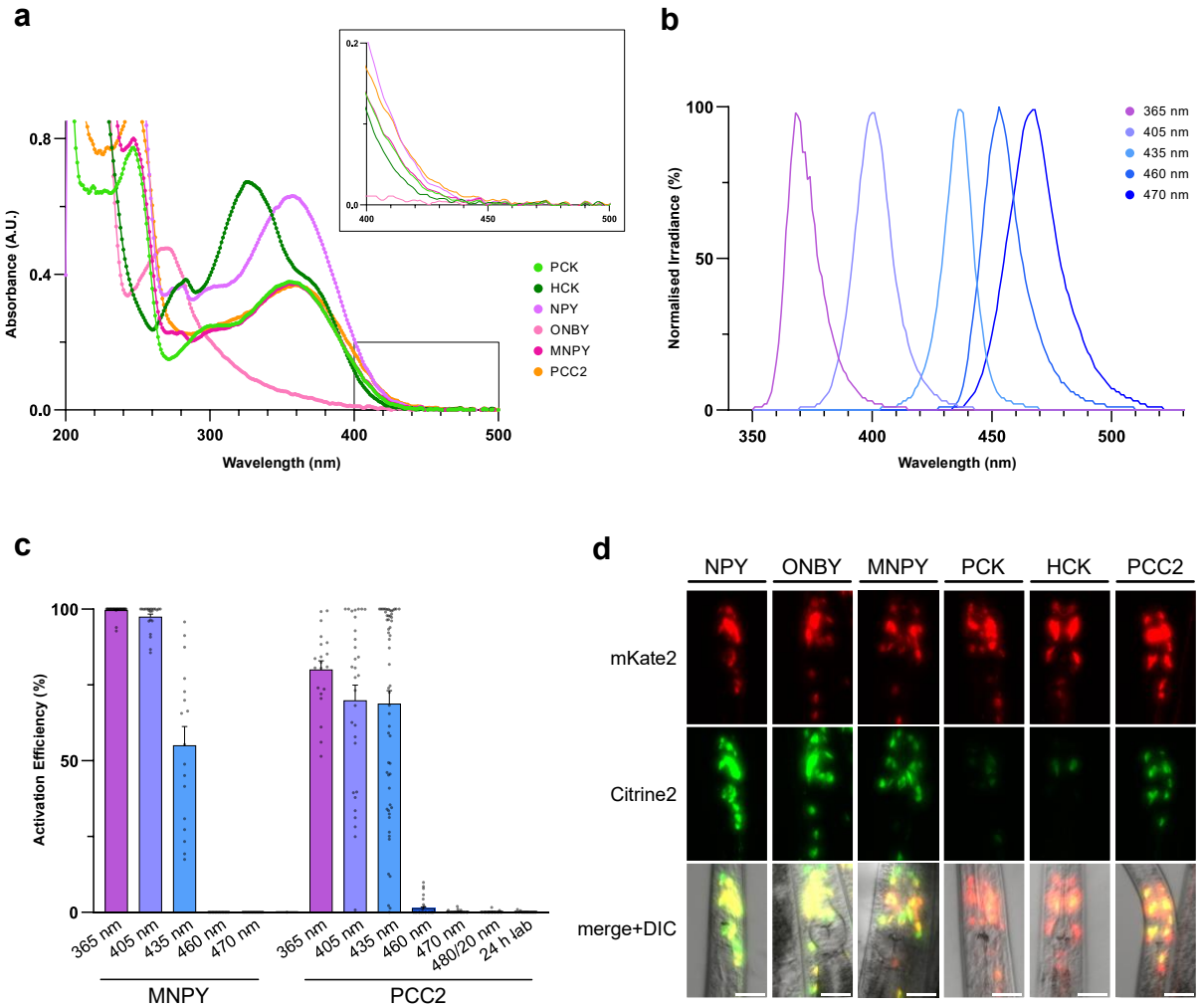

Supplementary Fig. 4 Activation of PC-FLP variants at higher wavelengths. a UV-vis absorbance of the different photocaged variants of tyrosine, lysine, and cysteine. **b** Relative irradiance of the "365 nm", "405 nm", "435 nm", "460 nm", "470 nm" LEDs from the pE-4000 light source (CoolLED). Spectra sourced from FPbase[1]. **c** Activation efficiency of animals expressing PC-FLP(Y343MNPY) and PC-FLP(C189PCC2) 24 hours after illumination by "365 nm", "405 nm", "435 nm", "460 nm", "470 nm" LEDs from the pE-4000 light source (CoolLED) for 5 minutes. Additionally, activation efficiency of animals expressing PC-FLP(C189PCC2) that were exposed to the output of the HXP120 light source (Leistungselektronik Jena)

through a 480/20 nm filter (Oxford Instruments Andor, MM-7253-GFP), and of worms that were left exposed to laboratory fluorescent lights for 24 hours. **d** Fluorescence microscopy of worms expressing the PC-FLP system using the different photocaged variants of tyrosine, lysine, and cysteine and activated using the 405 nm laser on a Zeiss LSM800 confocal microscope. Worms were grown in the presence of their respective ncAA at a concentration of 1 mM for 24 hours and illuminated with the 405 nm laser at 50% power. The worms were then imaged 24 hours after illumination. Scale bars represent: 20 µm.

Supplementary Table 1 Transgenic *C. elegans* strains.

Name	Description	Genetic Background	Expression Plasmids (µg)
SGR129	*greEx114[glr-1p::FLP(G5D)(K223TAG)::HA::egl-13NLS::SL2::mKate2; maco-1p::FRT_lacZ 3'UTR_FRT::Citrine2; sur-5p::HygR; glr-1p::smad-4NES::PCKRS(13IPYER); rpr-1p::tRNA(M15)]*	N2	KB438(6), KB454(2.5), JJ466(1.5), SE149(4.5)
SGR130	*greEx115[glr-1p::FLP(G5D)(K223TAG)::HA::egl-13NLS::SL2::mKate2; maco-1p::FRT_lacZ 3'UTR_FRT::Citrine2; sur-5p::HygR; glr-1p::smad-4NES::PCKRS(13IPYER); rpr-1p::tRNA(M15)]*	N2	KB438(6), KB454(2.5), JJ466(1.5), SE149(4.5)
SGR131	*greEx116[glr-1p::FLP(G5D)(K223TAG)::HA::egl-13NLS::SL2::mKate2; maco-1p::FRT_lacZ 3'UTR_FRT::Citrine2; sur-5p::HygR; glr-1p::smad-4NES::PCKRS(13IPYER); rpr-1p::tRNA(M15)]*	N2	KB438(6), KB454(2.5), JJ466(1.5), SE149(4.5)
SGR132	*greEx117[glr-1p::FLP(G5D)(K223TAG)::HA::egl-13NLS::SL2::mKate2; maco-1p::FRT_lacZ 3'UTR_FRT::Citrine2; sur-5p::HygR; glr-1p::smad-4NES::PCKRS(13IPYER); rpr-1p::tRNA(M15)]*	N2	KB438(6), KB454(2.5), JJ466(1.5), SE149(4.5)
SGR112	*greEx97[glr-1p::FLP(G5D)(Y343TAG)::HA::egl-13NLS::SL2::mKate2; maco-1p::FRT_lacZ 3'UTR_FRT::Chrimson::F2A::Citrine2; sur-5p::HygR; glr-1::Smad4::NPYRS; rpr-1p::tRNA(C15)]*	N2	KB463(6), KB454(2.5), AT11(1.5), SE150(4.5)
SGR122	*greEx107[glr-1p::FLP(G5D)(Y343TAG)::HA::egl-13NLS::SL2::mKate2; maco-1p::FRT_lacZ 3'UTR_FRT::Chrimson::F2A::Citrine2; sur-5p::HygR; glr-1::Smad4::NPYRS; rpr-1p::tRNA(C15)]*	N2	KB463(6), KB454(2.5), AT11(1.5), SE150(4.5)
SGR133	*greEx118[glr-1p::FLP(G5D)(C189TAG)::HA::egl-13NLS::SL2::mKate2; maco-1p::FRT_lacZ 3'UTR_FRT::Citrine2; sur-5p::HygR; glr-1p::smad-4NES::PCC2RS; rpr-1p::tRNA(M15)]*	N2	JJ543(6), KB454(2.5), JJ546(1.5), SE149(4.5)
SGR134	*greEx119[glr-1p::FLP(G5D)(C189TAG)::HA::egl-13NLS::SL2::mKate2; maco-1p::FRT_lacZ 3'UTR_FRT::Citrine2; sur-5p::HygR; glr-1p::smad-4NES::PCC2RS; rpr-1p::tRNA(M15)]*	N2	JJ543(6), KB454(2.5), JJ546(1.5), SE149(4.5)
SGR135	*greEx120[glr-1p::FLP(G5D)(C189TAG)::HA::egl-13NLS::SL2::mKate2; maco-1p::FRT_lacZ 3'UTR_FRT::Citrine2; sur-5p::HygR; glr-1p::smad-4NES::PCC2RS; rpr-1p::tRNA(M15)]*	N2	JJ543(6), KB454(2.5), JJ546(1.5), SE149(4.5)
SGR136	*greEx121[glr-1p::FLP(G5D)(C189TAG)::HA::egl-13NLS::SL2::mKate2; maco-1p::FRT_lacZ 3'UTR_FRT::Citrine2; sur-5p::HygR; glr-1p::smad-4NES::PCC2RS; rpr-1p::tRNA(M15)]*	N2	JJ543(6), KB454(2.5), JJ546(1.5), SE149(4.5)
SGR137	*greEx122[glr-1p::FLP(G5D)(C189TAG)::HA::egl-13NLS::SL2::mKate2; maco-1p::FRT_lacZ 3'UTR_FRT::Citrine2; sur-5p::HygR; glr-1p::smad-4NES::PCC2RS; rpr-1p::tRNA(M15)]*	N2	JJ543(6), KB454(2.5), JJ546(1.5), SE149(4.5)
SGR138	*greEx123[glr-1p::FLP(G5D)(K223TAG)::HA::egl-13NLS::SL2::mKate2; maco-1p::FRT_lacZ 3'UTR_FRT::Citrine2; sur-5p::HygR; glr-1p::smad-4NES::HCKRS; rpr-1p::tRNA(M15)]*	N2	KB438(6), KB454(2.5), JJ461(1.5), SE149(4.5)
SGR139	*greEx124[glr-1p::FLP(G5D)(K223TAG)::HA::egl-13NLS::SL2::mKate2; maco-1p::FRT_lacZ 3'UTR_FRT::Citrine2; sur-5p::HygR; glr-1p::smad-4NES::HCKRS; rpr-1p::tRNA(M15)]*	N2	KB438(6), KB454(2.5), JJ461(1.5), SE149(4.5)
SGR140	*greEx125[glr-1p::FLP(G5D)(K223TAG)::HA::egl-13NLS::SL2::mKate2; maco-1p::FRT_lacZ 3'UTR_FRT::Citrine2; sur-5p::HygR; glr-1p::smad-4NES::HCKRS; rpr-1p::tRNA(M15)]*	N2	KB438(6), KB454(2.5), JJ461(1.5), SE149(4.5)
SGR141	*greEx126[glr-1p::Cre(R119A)(Y324TAG)::HA::egl-13NLS::SL2::mKate2; maco-1p::loxP_lacZ 3'UTR_loxP::Citrine2; sur-5p::HygR; glr-1p::smad-4NES::NPYRS; rpr-1p::tRNA(M15)]*	N2	JJ191(6), KB462(2.5), AT11(1.5), SE149(4.5)

SGR142	*greEx127[glr-1p::Cre(R119A)(Y324TAG)::HA::egl-13NLS::SL2::mKate2; maco-1p::loxP_lacZ 3'UTR_loxP::Citrine2; sur-5p::HygR; glr-1p::smad-4NES::NPYRS; rpr-1p::tRNA(M15)]*	N2	JJ191(6), KB462(2.5), AT11(1.5), SE149(4.5)
SGR143	*greEx128[glr-1p::Cre(R119A)(K201TAG)::HA::egl-13NLS::SL2::mKate2; maco-1p::loxP_lacZ 3'UTR_loxP::Citrine2; sur-5p::HygR; glr-1p::smad-4NES::PCKRS(13IPYER); rpr-1p::tRNA(M15)]*	N2	KB389(6), KB462(2.5), JJ466(1.5), SE149(4.5)
SGR144	*greEx129[glr-1p::Cre(R119A)(K201TAG)::HA::egl-13NLS::SL2::mKate2; maco-1p::loxP_lacZ 3'UTR_loxP::Citrine2; sur-5p::HygR; glr-1p::smad-4NES::PCKRS(13IPYER); rpr-1p::tRNA(M15)]*	N2	KB389(6), KB462(2.5), JJ466(1.5), SE149(4.5)
SGR145	*greEx130[glr-1p::Cre(R119A)(K201TAG)::HA::egl-13NLS::SL2::mKate2; maco-1p::loxP_lacZ 3'UTR_loxP::Citrine2; sur-5p::HygR; glr-1p::smad-4NES::HCKRS; rpr-1p::tRNA(M15)]*	N2	KB389(6), KB462(2.5), JJ461(1.5), SE149(4.5)
SGR146	*greEx131[glr-1p::Cre(R119A)(K201TAG)::HA::egl-13NLS::SL2::mKate2; maco-1p::loxP_lacZ 3'UTR_loxP::Citrine2; sur-5p::HygR; glr-1p::smad-4NES::HCKRS; rpr-1p::tRNA(M15)]*	N2	KB389(6), KB462(2.5), JJ461(1.5), SE149(4.5)
SGR147	*greEx132[glr-1p::Cre(R119A)(K201TAG)::HA::egl-13NLS::SL2::mKate2; maco-1p::loxP_lacZ 3'UTR_loxP::Citrine2; sur-5p::HygR; glr-1p::smad-4NES::HCKRS; rpr-1p::tRNA(M15)]*	N2	KB389(6), KB462(2.5), JJ461(1.5), SE149(4.5)
SGR148	*greEx133[glr-1p::Cre(R119A)(K201TAG)::HA::egl-13NLS::SL2::mKate2; maco-1p::loxP_lacZ 3'UTR_loxP::Citrine2; sur-5p::HygR; glr-1p::smad-4NES::HCKRS; rpr-1p::tRNA(M15)]*	N2	KB389(6), KB462(2.5), JJ461(1.5), SE149(4.5)
SGR107	*greEx92[glr-1p::FLP(G5D)(K223TAG)::HA::egl-13NLS::SL2::mKate2; maco-1p::FRT_lacZ 3'UTR_FRT::Chrimson::F2A::Citrine2; rps-0p::HygR; glr-1::Smad4::PCKRS; rpr-1p::tRNA(C15)]*	N2	KB438(6), KB443(2.5), SE174(1.5), SE150(4.5)
SGR118	*greEx103[glr-1p::FLP(G5D)(K223)TAG::HA::egl-13NLS::SL2::mKate2; maco-1p::FRT_lacZ 3'UTR_FRT::Chrimson::F2A::Citrine2; rps-0p::HygR; glr-1::Smad4::PCKRS; rpr-1p::tRNA(C15)]*	N2	KB438(6), KB443(2.5), SE174(1.5), SE150(4.5)
SGR149	*greEx134[glr-1p::FLP(G5D)(Y343TAG)::HA::egl-13NLS::SL2::mKate2; maco-1p::FRT_lacZ 3'UTR_FRT::Chrimson::F2A::Citrine2; sur-5p::HygR; glr-1p::smad-4NES::NPYRS; rpr-1p::tRNA(M15)]*	N2	KB463(6), KB458(2.5), AT11(1.5), SE149(4.5)
SGR150	*greEx135[glr-1p::FLP(G5D)(C189TAG)::HA::egl-13NLS::SL2::mKate2; maco-1p::FRT_lacZ 3'UTR_FRT::Chrimson::F2A::Citrine2; sur-5p::HygR; glr-1p::smad-4NES::PCC2RS; rpr-1p::tRNA(M15)]*	N2	JJ546(6), KB458(2.5), JJ546(1.5), SE149(4.5)
SGR151	*greEx136[glr-1p::FLP(G5D)(C189TAG)::HA::egl-13NLS::SL2::mKate2; maco-1p::FRT_lacZ 3'UTR_FRT::Chrimson::F2A::Citrine2; sur-5p::HygR; glr-1p::smad-4NES::PCC2RS; rpr-1p::tRNA(M15)]*	N2	JJ546(6), KB458(2.5), JJ546(1.5), SE149(4.5)
SGR152	*greEx137[glr-1p::FLP(G5D)(C189TAG)::HA::egl-13NLS::SL2::mKate2; maco-1p::FRT_lacZ 3'UTR_FRT::Chrimson::F2A::Citrine2; sur-5p::HygR; glr-1p::smad-4NES::PCC2RS; rpr-1p::tRNA(M15)]*	N2	JJ546(6), KB458(2.5), JJ546(1.5), SE149(4.5)
SGR153	*greEx138[sur-5p::smad-4NES::PCKRS(wt); sur-5p::HygR; rps--0p::GFP(TAG)::mCherry::HA::egl-13NLS; rpr-1p::tRNA(M15)]*	smg-6(ok1794)	JJ518(2), SG88(3), SE149(6)
SGR154	*greEx139[sur-5p::smad-4NES::PCKRS(wt); sur-5p::HygR; rps--0p::GFP(TAG)::mCherry::HA::egl-13NLS; rpr-1p::tRNA(M15)]*	smg-6(ok1794)	JJ518(2), SG88(3), SE149(6)
SGR155	*greEx140[sur-5p::smad-4NES::PCKRS(13IPYER); sur-5p::HygR; rps-0p::GFP(TAG)::mCherry::HA::egl-13NLS; rpr-1p::tRNA(M15)]*	smg-6(ok1794)	JJ238(2), SG88(3), SE149(7)
SGR156	*greEx141[sur-5p::smad-4NES::PCKRS(13IPYER); sur-5p::HygR; rps-0p::GFP(TAG)::mCherry::HA::egl-13NLS; rpr-1p::tRNA(M15)]*	smg-6(ok1794)	JJ238(2), SG88(3), SE149(7)
SGR157	*greEx142[sur-5p::smad-4NES::PCKRS(13IPYER); sur-5p::HygR; rps-0p::GFP(TAG)::mCherry::HA::egl-13NLS; rpr-1p::tRNA(M15)]*	smg-6(ok1794)	JJ238(2), SG88(3), SE149(7)
SGR158	*greEx143[sur-5p::smad-4NES::HCKRS; sur-5p::HygR; rps--0p::GFP(TAG)::mCherry::HA::egl-13NLS; rpr-1p::tRNA(M15)]*	smg-6(ok1794)	JJ345(2), SG88(3), SE149(7)
SGR159	*greEx144[sur-5p::smad-4NES::HCKRS; sur-5p::HygR; rps--0p::GFP(TAG)::mCherry::HA::egl-13NLS; rpr-1p::tRNA(M15)]*	smg-6(ok1794)	JJ345(2), SG88(3), SE149(7)
SGR160	*greEx145[sur-5p::smad-4NES::HCKRS; sur-5p::HygR; rps--0p::GFP(TAG)::mCherry::HA::egl-13NLS; rpr-1p::tRNA(M15)]*	smg-6(ok1794)	JJ345(2), SG88(3), SE149(7)

Supplementary Table 2 Expression plasmids.

Plasmid Number	Description	Source Plasmids			
		Dest	p1	p2	p3
AT11	*glr-1p::HuSmad4::MmNPYRS::let858_3'UTR; sur-5p::HygR::unc-54_3'UTR*	SE80	IR157	KB126	SG606
JJ191	*glr-1p::Cre(R119A,Y324TAG)::HA::EGL-13_NLS::SL2::mKate2::let858_3'UTR*	PDESTII	IR157	JJ190	IR322
JJ238	*sur-5p::HuSmad4::MmPCKRS(13IPYER)::let858_3'UTR; sur-5p::HygR::unc-54_3'UTR*	SE80	SE72	JJ237	SG606
JJ345	*sur-5p::HuSmad4::MmHCKRS::let858_3'UTR; sur-5p::HygR::unc-54_3'UTR*	SE80	SE72	JJ338	SG606
JJ461	*glr-1p::HuSmad4::MmHCKRS::let858_3'UTR; sur-5p::HygR::unc-54_3'UTR*	SE80	IR157	JJ338	SG606
JJ466	*glr-1p::HuSmad4::MmPCKRS(13IPYER)::let858_3'UTR; sur-5p::HygR::unc-54_3'UTR*	SE80	IR157	JJ237	SG606
JJ518	*sur-5p::HuSmad4::PCKRS::let858_3'UTR; sur-5p::HygR::unc-54_3'UTR*	SE80	SE72	SE154	SG606
JJ543	*glr-1p::FLP(G5D,C189TAG)::HA::EGL-13_NLS::SL2::mKate2::let858_3'UTR*	PDESTII	IR157	JJ540	IR322
JJ546	*glr-1p::HuSmad4::MmPCC2RS::let858_3'UTR; sur-5p::HygR::unc-54_3'UTR*	SE80	IR157	KB124	SG606
KB389	*glr-1p::Cre(R119A,K201TAG)::HA::EGL-13_NLS::SL2::mKate2::let858_3'UTR*	PDESTII	IR157	SE17	IR322
KB438	*glr-1p::FLP(G5D,K223TAG)::HA::EGL-13_NLS::SL2::mKate2::let858_3'UTR*	PDESTII	IR157	KB257	IR322
KB443	*maco-1p::FRT::B-Gal_3'UTR::FRT::Chrimson::F2A::Citrine2::HA::let858_3'UTR*	PDESTII	SE77	LD222	KB431
KB454	*maco-1p::FRT::B-Gal_3'UTR::FRT::Citrine2::HA::let858_3'UTR*	PDESTII	SE77	LD222	KB442
KB458	*maco-1p::FRT::B-Gal_3'UTR::FRT::Chrimson::F2A::Citrine2::HA::egl-13::let858_3'UTR*	PDESTII	SE77	LD222	KB432
KB462	*maco-1p::loxp::B-Gal-3'UTR::loxp::Citrine2::HA::let858_3'UTR*	PDESTII	SE77	SG365	KB442
KB463	*glr-1p::FLP(G5D,Y343TAG)::HA::EGL-13_NLS::SL2::mKate2::let858_3'UTR*	PDESTII	IR157	KB321	IR322
SE149	*rpr-1p::M15(CUA)::sup-7_3'UTR*	[2]			
SE150	*rpr-1p::C15(CUA)::sup-7_3'UTR*	[3]			
SE174	*glr-1p::HuSmad4::MmPCKRS::let858_3'UTR; sur-5p::HygR::unc-54_3'UTR*	[3]			
SG88	*rps-0p::GFP::TAG::mCherry::HA::EGL-13_NLS::unc-54_3'UTR*	[4]			

Supplementary Table 3 Entry plasmids.

Plasmid Number	Description	Source
IR157	*glr-1p*	[3]
IR322	*SL2::mKate2::let858_3'UTR*	IR322 is identical to IR182[3] with an mKate2 gene in place of the GFP gene
JJ190	*Cre(R119A,Y324TAG)::HA::EGL-13_NLS*	Modified from SE17[3], K201TAG removed, and Y324TAG introduced with primers [(F) aacatcgtcatgaactagatccgtaacctcgactc, (R) ctagttcatgacgatgttgacgttg]
JJ237	*HuSmad4::MmPCKRS(13IPYER)*	Constructed by introducing mutations T13I, T56P, H62Y, A100E, S193R into SE154
JJ338	*HuSmad4::MmHCKRS*	Constructed by introducing mutations Y306A and L309M into HuSmad4::MmPylRS using primers [(F) CTCGCCAACTACATGCGTAAGCTCGACCGTGCC, (R) CATGTAGTTGGCGAGGTTTGGGGCGAGCATTG]
JJ540	*FLP(G5D,C189TAG)::HA::EGL-13_NLS*	Constructed by introducing C189TAG into KB258 FLP(G5D)::HA::egl-13 using primers [(F) catcaacTAGggacgtttctccgacatcaagaac, (R) gagaaacgtccCTAgttgatgaaggtggcgaggaag]
KB124	*HuSmad4::MmPCC2RS*	[2]
KB126	*HuSmad4::MmNPYRS*	Identical to KB125[5], but with HuSmad4 instead of Pkiα
KB257	*FLP(G5D,K223TAG)::HA::EGL-13_NLS*	Constructed by introducing G5D mutation into SE13 FLP(K223TAG)::HA::egl-13 using primers [(F)

		acaattcgACatcctctgcaagaccccaccaaag, (R) cttgcagag-gatGTcgaattgtggcatttttagcctg]
KB321	*FLP(G5D,Y343TAG)::HA::EGL-13_NLS*	Constructed by introducing Y343TAG into KB258 FLP(G5D)::HA::egl-13 using primers [(F) gtaccaccTAGac-ccaccaaatcaccgccatcccagac, (R) gatggcggtgattt-ggtgggtCTAggtggtacgggcgacggcggaggcacgcttg]
KB431	*Chrimson::F2A::Citrine2::HA::let858_3'UTR*	Constructed by Nebuilder between amplification of Chrimson::Citrine2::let-858_3'UTR using primers [(F) GTCGAGTCCAACCCAGGACCAATGGTATCGAAAGGa-GAGG, (R) TGCTTGACTCCGGATCCTGGGACTG-TATCCTCATCTTCCTC] and oligonucleotide [TGGTCCTGGGTTGGACTCGAC-GTCTCCGGCGAGCTTGAGGAGGTCGAAGTT-GAGGGTTTGCTTGACTCCGGATCCTGG] to introduce the F2A
KB432	*Chrimson::F2A::Citrine2::HA::egl-13::let858_3'UTR*	Constructed by introducing egl-13 into KB431 using pri-mers [(F) TCCGACAAAACTGAGTGAAAACGCGAAGAA-GCTTGCCAAGGAAGTTGAAAATtaac-gtgaagtggaatcggatgatcgacgccg, (R) GCTTCTTCGCGTTTTCACTCAGTTTTGTCGGAT-TCGCTTTTCGTCTACGGCTCATAGCGTAG-TCTGGGACATCATATGGGTA]
KB442	*Citrine2::HA::let858_3'UTR*	Constructed by BP reaction into pDONR P2r-P3 of frag-ment generated by PCR from Chrimson::Citrine2::let-858_3'UTR using primers [(F) GGGGACAGCTTTCTT-GTACAAAGTGGTAAAAAAATGGTATCGAAAGGAGAG-GAATTATTTACTG, (R) GGGGACAACTTTGTATAA-TAAAGTTGatacggattcgcatttgccaag]
LD222	*FRT::B-Gal_3'UTR::FRT*	Constructed by BP reaction into pDONR221 of fragment generated by PCR from SG365 loxp::B-Gal-3'UTR::loxp using primers [(F) GGGGACAAGTTTGTACAAAAAA-GCAGGCTgaagttcctatactttctagagaa-taggaacttcggaataggaacttcATGGTCGTTTTACAACGTCGT GACTGGGAAAACCC, (R) GGGGACCACTTTGTACAA-GAAAGCTGGGTgaagttcctattccgaagttcctattctcta-gaaagtataggaacttcGTTTCATGTTTCAAAAAAAATTTATT CTTTATTCTTTATTAGATCCTATTATTTTTGACACCAG-ACAAGTTGGTAATGGTAGC] using SG365 (Davis2021) as a template
SE154	*HuSmad4::PCKRS*	[3]
SE17	*Cre(R119A,K201TAG)*	[3]
SE72	*sur-5p*	[3]
SE77	*maco-1p*	[3]
SE80	*sur-5p::HygR::unc-54_3'UTR*	Constructed from IR98[3] by replacing the rps-0p::HygR::unc-54_3'UTR with sur-5p::HygR::unc-54_3'UTR by ligation using restriction enzymes KasI and AscI
SG365	*loxp::B-Gal-3'UTR::loxp*	[3]
SG606	*let858_3'UTR*	[3]

SUPPLEMENTARY REFERENCES

1. Lambert, T. J. FPbase: a community-editable fluorescent protein database. *Nat Methods* **16**, 277–278 (2019).
2. Xi, Z. *et al.* Using a quadruplet codon to expand the genetic code of an animal. *Nucleic Acids Research* **50**, 4801–4812 (2022).
3. Davis, L. *et al.* Precise optical control of gene expression in C elegans using improved genetic code expansion and Cre recombinase. *eLife* **10**, e67075 (2021).
4. Greiss, S. & Chin, J. W. Expanding the Genetic Code of an Animal. *J. Am. Chem. Soc.* **133**, 14196–14199 (2011).

5. O'Shea, J. M. *et al.* Generation of Photocaged Nanobodies for Intracellular Applications in an Animal Using Genetic Code Expansion and Computationally Guided Protein Engineering**. *ChemBioChem* **23**, e202200321 (2022).